Urban geophysics and the potential for the basin edge-effect in the Wellington CBD

T.A. Stern, S. B. Thorpe-Loversuch[1] , A.I. Stronach[2]

Earth Sciences, Victoria University of Wellington, New Zealand, 1- now at WSP, 2-Now at RDCL

W.R. Stratford.

GNS, Science, Lower Hutt, New Zealand

ABSTRACT

Many of our cities are built within sedimentary basins. Both the depth and geometric shape of a basin will influence, and generally enhance the level of shaking during earthquakes. Our focus is the Wellington CBD, where we use seismic reflection and gravity methods to assess the depth and shape of the basin beneath the city. An initial gravity survey of the Wellington CBD is interpreted to show sedimentary thicknesses of up to 450 m in the CentrePort area, and 200 m in much of Thorndon. These values are higher than previous estimates. The gravity survey of the Wellington CBD also highlights the importance of the subsurface expression of the Lambton Fault for ground shaking. The fault strikes northeast beneath the railyards, and dips steeply to the southeast to form the effective geophysical edge of the Wellington Basin. We show that the subsurface expression of the Lambton Fault has the potential to create an edge-effect whereby strong amplification of ground motion may cause focussed damage along a narrow corridor just inboard, or east of, its surface trace.

1 INTRODUCTION

Sedimentary basins, which are a favoured place to build cities because they are flat, can become a natural resonant chamber during earthquakes (Rial et al., 1992). This was underscored by the Kaikoura earthquake, which although ~80 km from Wellington, produced sustained shaking within the CBD caused by surface waves that became trapped and amplified (Bradley et al., 2017). Mapping of the 3D structure of the Wellington sedimentary basin is, therefore, critical for seismic hazard assessment of the city.

Mapping depth to bedrock in the Wellington CBD was initially based on bore holes drilled to basement and passive seismic methods (Semmens et al., 2010). Further refinements and application of surface wave dispersion brought about changes from this initial model (Fig.1c), (Kaiser et al., 2019; Vantassel et al., 2018), yet the results are not consistent (Table 1). Estimates from three localities demonstrate this divergence: the SW corner of CentrePort wharf, the log yards at CentrePort and Waitangi Park in Te Aro (Fig.1).

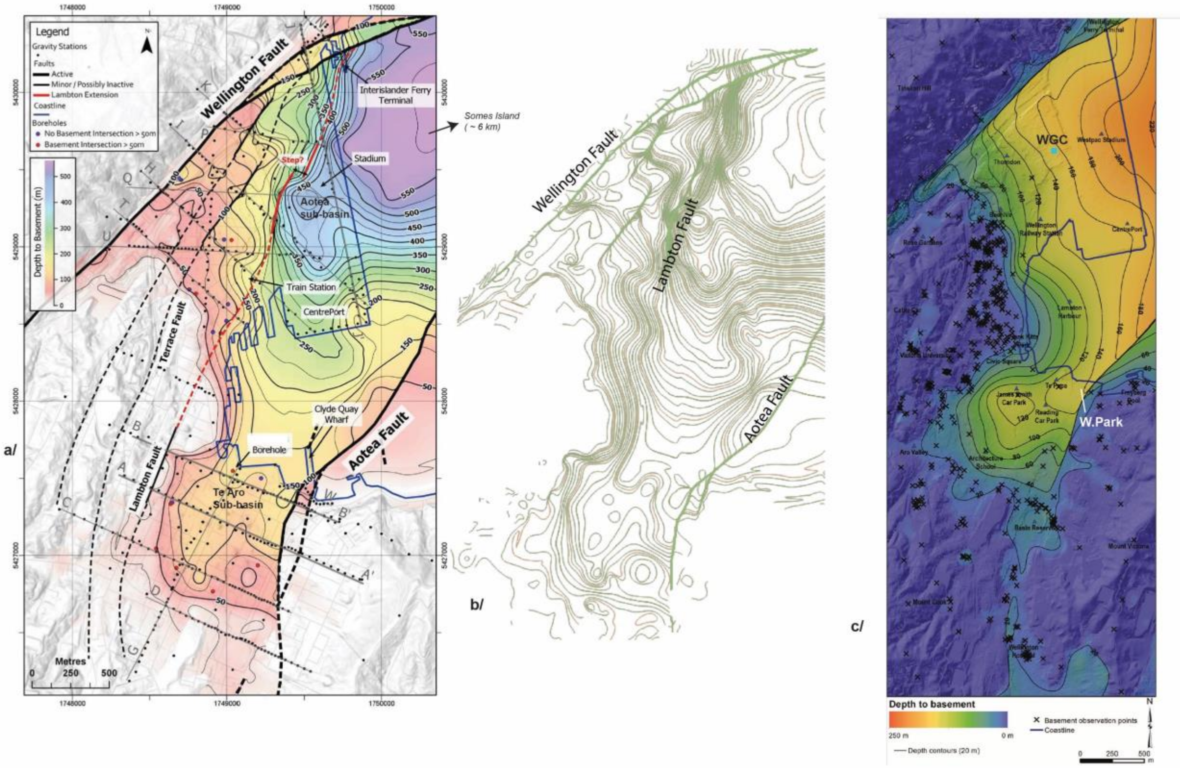

Figure 1. a/ Contours of depth to basement based on gravity model of Stronach & Stern (2021). Contour interval = 25. b/ Contours of sediment thickness at 10 m interval based on a. showing dominant effect of subsurface expression of Lambton fault. c/ Previous basement map of Kaiser et al (2019) discussed in text. Locations for Wellington Girls College (WGC) and Waitangi Park (W.Park) are marked.

DEPTHS TO BASEMENT	**SW corner of CP(CentrePort)**	**Log yard of CP**	**Waitangi Park- Te Aro**
Semmens et al	160	200	40
Vantassel et al (2018)	116	392	-
Kaiser et al (2019)	140	200	140
Stronach and Stern (2021)	250	450	160

Maximum Per cent difference	215%	225%	400%

Table1: Depth estimates for depth to basement within the Wellington CBD.

There is no consistent pattern in the divergence of these estimates apart from the gravity-based estimates (Stronach and Stern, 2021) being consistently deeper. The largest difference is at Waitangi Park, Te Aro, (Fig.1) where the estimates differ by a factor of 400%. All methods used in gaining basin depths (Table 1) have associated caveats and inherent uncertainties, and therefore a more direct and more robust method is needed to establish basement depths in urban areas like Wellington. We suggest active-source seismic-reflection is this method, as it is widely used for exploration of sedimentary basins, especially in the oil and gas industry (Allen and Allen, 2005).

In a companion paper (Thorpe-Loversuch et al. 2024) we outline initial results of seismic reflection studies at three localities within the Wellington basin. In this study we bring gravity and seismic studies together to provide a new perspective of the subsurface geometry of the Wellington basin. In particular, we show that the effective western edge of the basin is different to previously mapped, and demonstrate through simple 2D modelling with dimensionless variables, that this edge could be responsible for amplified shaking in the Thorndon-Pipitea region of the Wellington CBD.

2 GEOPHYSICAL METHODS

2.1- Gravity surveying

A gravity survey of the Wellington CBD was carried out in 2019 with a Scintrex™ CG6 gravimeter (Stronach and Stern, 2021). Conventional terrain and elevation corrections were applied, and corrections for the gravitational attraction of buildings were also undertaken using an established method (Yu, 2014). Parts of the city like the railway yards were difficult to access for safety and security reasons, but the road network provided a reasonable coverage. Data were interpreted along 2D lines then the structures contoured to make a 3D map (Figs.1a,b).

Distinguishing features of the gravity anomaly inversion model, compared to previous structural models (Kaiser et al., 2019; Semmens et al., 2010), are the greater predicted depths to basement and the different basin shape (Figs.1b, c). Previous maximum depths in the Sky-Stadium-CentrePort region were about 200 m, whereas the gravity inversion suggests depths >400 m. Depth resolution from gravity inversion is, however, subject to uncertainty because of incomplete knowledge of the density contrast variation between basement rock and the sediment. Estimates of uncertainty are typically $\pm$ 10% and 20% for shallower and deeper directions, respectively ((Stronach and Stern, 2021). What the gravity method is good at, however, is resolving the shape and edge of subsurface masses, and in particular for this study the dominant subsurface expression of the Lambton fault.

Although the western edge of the basin was shown in earlier studies to be adjacent to the Wellington fault and alongside the Tinakori Hill (Kaiser et al., 2019; Semmens et al., 2010), the gravity data clearly show the largest change in subsurface relief occurs at a southeast-dipping surface whose surface projection is at a high angle to the Wellington Fault (Fig.1b), and defines a line that runs roughly parallel to the trace of the earlier recognised Lambton fault (Fig.1a, (Begg and Mazengarb, 1996; Grant-Taylor, 1963). This is important because of the basin edge effect (Adams et al., 1999; Ayoubi et al., 2021) that will be discussed shortly.

2.2 Seismic methods

In a companion paper to this (Thorpe-Loversuch et al.) we outline a programme of shear-wave seismic reflection work in the Wellington CBD. P-wave seismic reflection has dominated the exploration sector for decades because of its higher wave speeds and higher frequency. But shear-wave (or S-wave) surveys are useful in urban environments because better resolution is afforded by the shorter wavelength used (Pugin et al., 2004). As wavelength (λ) = velocity/frequency this may seem counter initiative as P-waves are always higher frequency than S-waves. However, the lower wave-speed of V_s tends to dominate (Table 2). For a S-wave basement reflection, frequency, wavelength and wave-speed in the overlying sedimentary unit are all lower than the P-wave equivalent. This means these S-waves are better suited to resolving a relatively thin layer (Chopra et al., 2006), and the seismic section will be longer in travel time, and the waveforms more drawn out so that the eye can resolve more features. Other studies (Harris, 2009) also highlight this relationship between the wavelength and frequency of P- an S-wave reflections from a common interface.

	P wave	**S-wave**
Period	23 msecs	40 msec
Frequency	43 Hz	25 Hz
Velocity	2000 m/s	550 m/s
Wavelength	46.5 m	22 m

Table 2: Frequency, velocity, and wavelength characteristics of phases on shot gather of Fig.2 for P and S-waves travelling in the sediments above basement.

The shot gather of Fig. 2 shows the rich spectrum of seismic phases that can be created by an accelerated weight drop recorded by horizontal geophones, rather than standard vertical geophones. These include refracted P and S through the near surface layers, P-wave reflections from basement at about 200 msec, surface waves, and S-wave reflections from the basement. All the P-wave information is contained within the top 200 msec of the record, which is also partly over printed by near surface P-wave refraction phases.

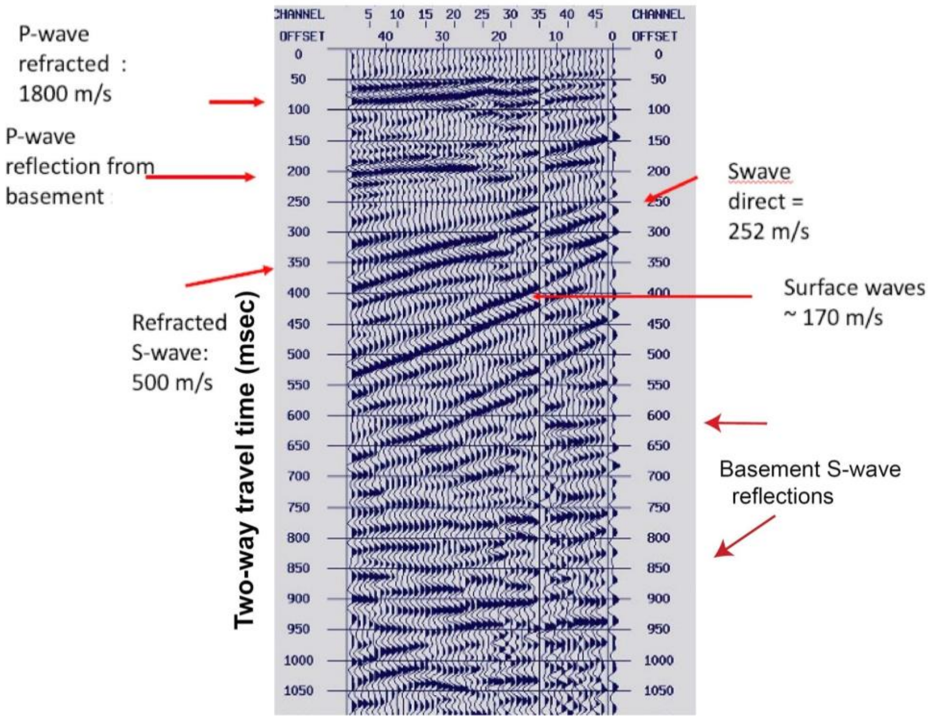

Figure 2. Shot gather from WGC using mechanical weight drop recorded by horizontal geophones. Spacing between phones = 1 m and first phone (phone #48) is offset from shot by 48 m. P and S - phases are identified and labelled. Note the P-wave basement reflector would be at depth of ~180 m for average P-wave speed in sediments of 1800 m/s. Likewise the S-wave basement reflector would be at depth of ~180 m for S-wave speed of 550 m/s.

On the other hand, the S-wave reflections are spread over 1000 msec of record but are contaminated by strong surface waves. However, processing methods in the F-K (time frequency- spatial frequency (K)) plane (Kearey and Brooks, 1991) allows us to remove steeply dipping events like the surface wave, thus making S-wave reflection analysis most suitable for shallow (~200 m deep) basins.

As reported in the companion paper we report on two sites: Wellington Girls' College (WGC) and Waitangi Park, where seismic reflection data are used to determine depth to basement. Both sites were chosen because of the need for a grassed strip at least 75 m long to carry out the survey. Maximum basin depths of 180 and 220 m (uncertainty of ± 5-10%), respectively, are reported. These depths are larger than those from 3D structural models for Wellington basin based on other means (See Table 1).

3.0 Amplification of ground motion – a dimensionless variables approach

A key outcome of the gravity survey discussed above was the new discovery of the structural basin edge seen in the subsurface striking along a line coincident with the Lambton Fault (Fig.1b). The existence of this edge raises the question of basin edge-effects (Kawase, 1996). This is the phenomenon where enhanced amplification of the ground motion occurs near the edge of a basin (Fig.3) due to constructive interference of trapped, vertically propagating waves, diffractions from the basin's internal corner, and horizontally travelling surface waves (Ayoubi et al., 2021). Globally, this is well documented with examples from the USA (Graves et al., 1998), Japan (Kawase, 1996), Turkey (Bakır et al., 2002) and New Zealand (Adams et al., 2003; Newton et al., 2022).

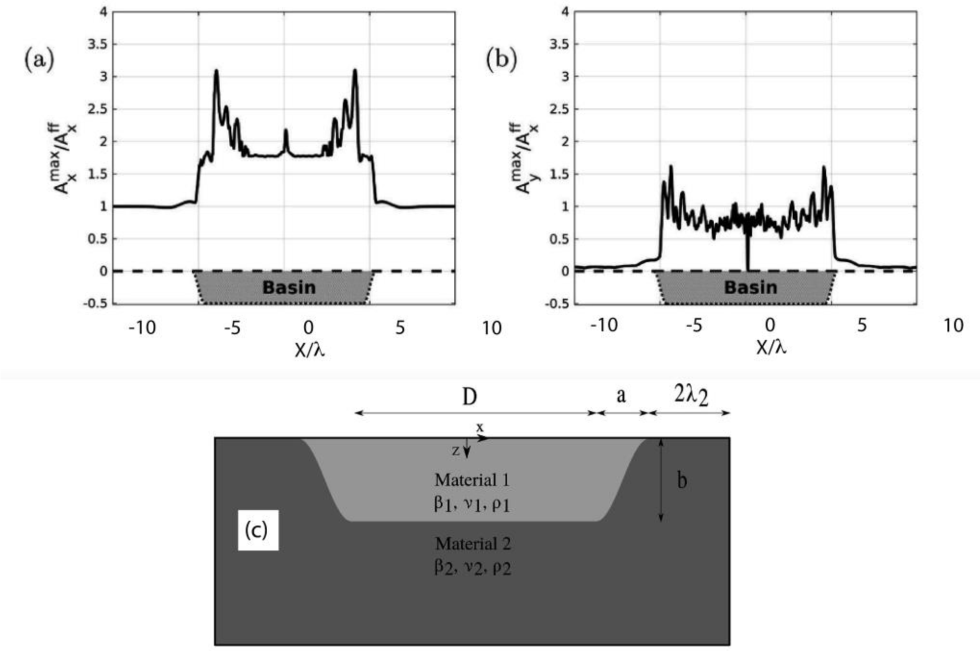

Figure 3: Template model for the dimensionless analysis of basin edge-effects (Ayoubi et al ,2021), for a vertically propagating Sv wave of Ricker type. Input dimensionaless ratios are gven in the first four lines of table 3. a/ shows the horizontal amplification normalised to ground motion two wavelengths distant from the edge of the basin. b/ as for a. but vertical motion. c/ simple two layer model with isotropic properties showing geometrical parameters a, b and D. Physical properties β, ν, ρ, and λ are shear wave speed, Poisson's ratio, density and seismic wavelength, respectively.

There are many unconstrained parameters needed to model shaking in basins (Benites and Olsen, 2005), and it can be challenging to isolate what is important and what is not. Useful insight into the basin edge-effect can be achieved by adopting a dimensionless analysis approach (Zohuri, 2015) that allows one to reduce the key drivers of the process to a few simple dimensionless ratios. A single output model can then act as a template that is scaled to the situation appropriate to the user. We follow a predetermined model (Ayoubi et al., 2021), that approximates the Wellington basin setting and gives maximum basin edge effects in both horizontal and vertical ground amplification (Fig. 3).

The input model is a steep-sided, 2D model parametrised by β, ν, and ρ (shear-wave speed, Poisson's ratio and density, respectively), for the sedimentary and basement rock layers. Four dimensionless ratios are specified for the output of fig.3: dimensionless slope, wave speed, frequency, and width (Table 3). We then specify an input frequency and solve for the geometric shape of the basin given by the quantities a, b, and D.

Input	Description	values
a/b	Dimensionless slope	3.6
$\beta_1/\ \beta_2$	Dimensionless wave speed	6.4
$\eta = f_0 b/\beta_1$	Dimensionless frequency	0.31
$(D+2a)/\lambda$	Dimensionless width	11.15
	Derived values for: f_0 = 0.7 Hz (Aotea)	
β_1, β_2	Shear wave speed, layers 1 and 2	550, 3520 (m/s)
a,b	Lateral extent and depth of sloping boundary (and basin)	876, 243 (m)
$\lambda = \beta_1/f_0$	Dominant wavelength in sediments	785 m
D	Dominant width of basin	7007 m
	Derived values for: f_0 = 1.5 Hz (Te Aro)	
β_1, β_2	Shear wave speed, layers 1 and 2	500, 3200 (m/s)
a,b	Lateral extent and depth of sloping boundary (and basin)	372, 103 (m)
$\lambda = \beta_1/f_0$	Dominant wavelength in sediments	333 m
D	Dominant width of basin	3000 m

Table 3. Inputs and predictions for analysis of Fig.3 and as discussed in text. Dimensionless quantities are given (Ayoubi et al., 2021) and produce ground motion amplification shown in Fig.3. Derived values of basin dimensions for given dominant frequencies appropriate for Aotea and Te Aro regions of Wellington CBD (Manea et al., 2024) are shown.

There are two distinct parts to the Wellington Basin: Te Aro and Aotea sub-basins (Fig.1a) with respective dominate vibration frequencies of 0.7 and 1.5 Hz (Manea et al., 2024). Te Aro is a confined basin, defined by the Aotea and Lambton faults, and is about 1.5 km wide with a maximum depth of 200 m. Aotea is the area of the CentrePort and opens to the harbour with the effective eastern margin of the basin being the submarine basement ridge that emerges as Somes Island (Fig.1a). The distance from the Lambton fault to the centre of Somes Island is 7.5 km. The basin here has maximum depth of ~400 m (Fig.1a).

Insertion of fundamental frequencies of $f_0 = 0.7$ and 1.5 Hz gives the predicted geometries shown in Table 3. Of note is that predicted geometry for the Aotea sub-basin is close to what is observed, but the width of the Te Aro basin is overestimated by 100%. For both cases the average basin depth predicted is half the maximum depth.

Nevertheless, our analysis suggests that the difference in the fundamental periods seen in the Wellington CBD may be influenced by both the effective basin depth and width. In addition, the model predicts a zone of strong ground-motion amplification to be linked in the zone directly above, and slightly inboard, of the subsurface expression of the Lambton fault as defined by the gravity inversion in Fig. 1b. However, the caveat is that the analysis is simple, as it is 2D and based on assuming a two-layer geometrical model.

4.0 Summary

In this study we demonstrate the utility for merging gravity and active source seismic methods to understand the structure and seismic hazard of urban areas built on complex sedimentary basins like Wellington City. These two geophysical methods complement each other as gravity gives reliable control on the shape of the subsurface basin, while seismic reflection provides robust depth estimates with uncertainties of the order of ±10%. We show that the subsurface structure of the Lambton fault has the potential to create an edge-effect whereby strong amplification of ground motion may cause focussed damage along a narrow corridor just inboard, or east of, its surface trace. The damage caused during earthquakes may be unexpectedly high in discrete areas of basin if the 3D subsurface structure is not correctly included in predictive shaking models.

Acknowledgement: We thank EQC for support of the gravity survey, and Victoria University and QuakeCore for support of the seismic work reported in this study.

Adams, B., Davis, R., Berrill, J., and Taber, J., 1999, Two-dimensional site effects in Wellington and the Hutt Valley- similarities to Kobe: University of Canterbury, Civil Engineeriung Research Report, 99-3.

Adams, B. M., Osborne, N. M., and Taber, J. J., 2003, The basin-edge effect from weak ground motions across the fault-bounded edge of the Lower Hutt Valley, New Zealand: Bulletin of the Seismological Society of America, v. 93, no. 6, p. 2703-2716.

Allen, P. A., and Allen, J. R., 2005, Basin Analysis, Oxford, Blackwell, 547 p.:

Ayoubi, P., Mohammadi, K., and Asimaki, D., 2021, A systematic analysis of basin effects on surface ground motion: Soil Dynamics and Earthquake Engineering, v. 141, p. 106490.

Bakır, B. S., Özkan, M. Y., and Cılız, S., 2002, Effects of basin edge on the distribution of damage in 1995 Dinar, Turkey earthquake: Soil Dynamics and Earthquake Engineering, v. 22, no. 4, p. 335-345.

Begg, J. G., and Mazengarb, C., 1996, The geology of the Wellington Area, scale 1:50,000: IGNS Ltd., Lower Hutt.

Benites, R., and Olsen, K. B., 2005, Modeling Strong Ground Motion in the Wellington Metropolitan Area, New Zealand: Bulletin of the Seismological Society of America, v. 95, no. 6, p. 2180-2196.

Bradley, B., Wotherspoon, L., and Kaiser, A., 2017, Ground motion and site effect observations in the Wellington region from the 2016 Mw 7.8 Kaikoura, New Zealand earthquake: Bull NZ Soc Earthquake Engineering, v. 50, no. 2, p. 94-105.

Chopra, S., Castagna, J., and Portniaguine, O., 2006, Seismic resolution and thin-bed reflectivity inversion: Canadian Society of Exploration Geophysicists Recorder, v. 1.

Grant-Taylor, T. L., 1963, Geological faults in the Wellington area New Zealand Institute of Architects Journal, v. 30, p. 68-69.

Graves, R. W., Pitarka, A., and Somerville, P. G., 1998, Ground-motion amplification in the Santa Monica area: Effects of shallow basin-edge structure: Bulletin of the Seismological Society of America, v. 88, no. 5, p. 1224-1242.

Harris, J. B., 2009, Hammer-impact SH-wave seismic reflection methods in neotectonic investigations: General observations and case histories from the Mississippi Embayment, U.S.A: Journal of Earth Science, v. 20, no. 3, p. 513-525.

Kaiser, A., Bourguignon, S., Hill, M., Wotherspoon, L., Bruce, Z., Morgenstern, R., and Giallini, S., 2019, Updated 3D basin model and the NZS 1170.5 subsoil class and site periods maps for the Wellington CBD: project 2017-GNS_03_NHRP: GNS consultancy Report 2019/01.

Kaiser, A. E., Hill, M. P., de la Torre, C., Bora, S., Manea, E., Wotherspoon, L., Atkinson, G. M., Lee, R., Bradley, B., Hulsey, A., Stolte, A., and Gerstenberger, M., 2023, Overview of Site Effects and the Application of the 2022 New Zealand NSHM in the Wellington Basin, New Zealand: Bulletin of the Seismological Society of America, v. 114, no. 1, p. 399-421.

Kawase, H., 1996, The Cause of the Damage Belt in Kobe: “The Basin-Edge Effect,” Constructive Interference of the Direct S-Wave with the Basin-Induced Diffracted/Rayleigh Waves: Seismological Research Letters, v. 67, no. 5, p. 25-34.

Kearey, P., and Brooks, M., 1991, An introduction to Geophysical Exploration, Oxford, Blackwell Scientific Publications.

Manea, E. F., Kaiser, A., Hill, M., Wotherspoon, L., Bourguignon, S., Bora, S., and Stolte, A., 2023, A High-Resolution Site Amplification Map for Wellington, New Zealand: Seismological Research Letters, v. 95, no. 1, p. 159-171.

Manea, E., Kaiser, A., Wotherspoon, L., Stolte, A., and Hill, M., 2022, Evaluation of site parameters to inform seismic site characterization in New Zealand Australian Earthquake Engineering Society 2022 National Conference, 24-25 November 2022 Mount Macedon, Victoria, Australia p. 9.

Newton, M., Louie, J. N., Stern, T., and Pancha, A., 2022, Low frequency non-ergodic synthetic modelling of earthquake basin effects in Welington, New Zealand, Poster, Southern California Earthquake Centre, Annual workshop.

Pugin, A. J. M., Larson, T. H., Sargent, S. L., McBride, J. H., and Bexfield, C. E., 2004, Near-surface mapping using SH-wave and P-wave seismic land-streamer data acquisition in Illinois, U.S: The Leading Edge, v. 23, no. 7, p. 677-682.

Rial, J. A., Saltzman, N. G., and Ling, H., 1992, Earthquake-Induced Resonance in Sedimentary Basins: American Scientist, v. 80, p. 566-578.

Semmens, S., Dellow, G. D., and Perrin, N. D., 2010, It’s our Fault-Geological and Geotechnical characterisation of the Wellington Central Business District: GNS Consultancy Report 2010/176.

Stronach, A., and Stern, T., 2021, A new basin depth map of the fault-bound Wellington CBD based on residual gravity anomalies: New Zealand Journal of Geology and Geophysics, p. 1-15, DOI: 10.1080/00288306.2021.2000438

Vantassel, J., Cox, B., Wotherspoon, L., and Stolte, A., 2018, Mapping Depth to Bedrock, Shear Stiffness, and Fundamental Site Period at CentrePort, Wellington, Using Surface-Wave Methods: Implications for Local Seismic Site AmplificationMapping Depth to Bedrock, Shear Stiffness, and Fundamental Site Period at CentrePort: Bulletin of the Seismological Society of America, v. 108, no. 3B, p. 1709-1721.

Yu, D., 2014, The influence of buildings on urban gravity surveys: Journal of Environmental and engineering geophysics, v. 19, p. 157-164.

Zohuri, B., 2015, Dimensional Analysis and Self-Similarity Methods for Engineers and Scientists, Springer International Publishing.